Tracing the origin of suspended sediment in a large Mediterranean river by combining continuous river monitoring and measurement of artificial and natural radionuclides

Mathilde Zebracki, Frédérique Eyrolle-Boyer, O. Evrard, David Claval, Brice Mourier, Stéphanie Gairoard, Xavier Cagnat, Christelle Antonelli

Tracing the origin of suspended sediment in a large Mediterranean river by combining continuous river monitoring and measurement of artificial and natural radionuclides

Mathilde Zebracki[1]*, Frédérique Eyrolle-Boyer[1], Olivier Evrard[2], David Claval[1], Brice Mourier[3,4], Stéphanie Gairoard[5], Xavier Cagnat[6], Christelle Antonelli[1]

[1]Laboratoire d'Etudes Radioécologiques en milieu Continental et Marin (LERCM), Institut de Radioprotection et de Sûreté Nucléaire (IRSN), Saint-Paul-lez-Durance, France
[2]Laboratoire des Sciences du Climat et de l'Environnement (LSCE/IPSL), Unité Mixte de Recherche 8212 (CEA/CNRS/UVSQ), Gif-sur-Yvette, France
[3]Université Lyon 1, UMR 5023 Ecologie des Hydrosystèmes Naturels et Anthropisés, ENTPE, CNRS, 3, Rue Maurice Audin, F-69518 Vaulx-en-Velin, France
[4]Université de Limoges, GRESE, EA 4330, 123 avenue Albert Thomas, 87060 Limoges, France
[5]Centre de Recherche et d'Enseignement de Géosciences de l'Environnement (CEREGE), Unité Mixte 34 (AMU/CNRS/IRD), Aix-en-Provence, France
[6]Laboratoire de Mesure de la Radioactivité dans l'Environnement (LMRE), Institut de Radioprotection et de Sûreté Nucléaire (IRSN), Orsay, France
*Corresponding author: zebracki@free.fr

ABSTRACT

Delivery of suspended sediment from large rivers to marine environments has important environmental impacts on coastal zones. In France, the Rhone River (catchment area of 98,000 km²) is by far the main supplier of sediment to the Mediterranean Sea and its annual solid discharge is largely controlled by flood events. This study investigates the relevance of alternative and original fingerprinting techniques based on the relative abundances of a series of radionuclides measured routinely at the Rhone River outlet to quantify the relative contribution of sediment supplied by the main tributaries during floods. Floods were classified according to the relative contribution of the main subcatchments (i.e., Oceanic, Cevenol, extensive Mediterranean and generalised). Between 2000 and 2012, 221 samples of suspended sediment were collected at the outlet and were shown to be representative of all flood types that occurred during the last

decade. Three geogenic radionuclides (i.e., ^{238}U, ^{232}Th and ^{40}K) were used as fingerprints in a multivariate mixing model in order to estimate the relative contribution of the main subcatchment sources – characterised by different lithologies - in sediment samples collected at the outlet. Results showed that total sediment supply originating from Pre-Alpine, Upstream, and Cevenol sources amounted to 10, 7 and 2.10^6 tons, respectively. These results highlight the role of Pre-Alpine tributaries as the main sediment supplier (53 %) to the Rhone River during floods. Other fingerprinting approaches based on artificial radionuclide activity ratios (i.e., $^{137}Cs/^{239+240}Pu$ and $^{238}Pu/^{239+240}Pu$) were tested and provided a way to quantify sediment remobilisation or the relative contributions of the southern tributaries. In future, fingerprinting methods based on natural radionuclides should be further applied to catchments with heterogeneous lithologies. Methods based on artificial radionuclides should be further applied to catchments characterised by heterogeneous post-Chernobyl ^{137}Cs deposition or by specific releases of radioactive effluents.

1 Introduction

Delivery of suspended sediments from large rivers to marine environments has important environmental impacts on coastal zones, where it modifies water quality, estuarine geomorphology and biogeochemical cycles (Syvitski et al. 2005; Meybeck and Vörösmarty 2005; Meybeck et al. 2007; Durrieu de Madron et al. 2011). Furthermore, the quality of riverine suspended sediment is impacted by human activities in the river catchment, and sediments may transport various particle-reactive contaminants from their sources within the catchment and convey them into marine environments (Durrieu de Madron et al. 2011; Fohrer and Chicharo 2011).

The magnitude of this impact is controlled by the sediment discharge of rivers that is strongly variable throughout time (Meybeck et al. 2003). In France, the Rhone River is by far the main supplier of sediment to the marine environment (Delmas et al. 2012).

The Rhone River supplies almost two-thirds of the total river discharge into the western Mediterranean Sea (Ludwig et al. 2009), delivering together with the Po River the most important input of suspended sediment to the Mediterranean Sea (Syvitski and Kettner 2007). It delivers more than 80 % of the particulate inputs to

the Gulf of Lions (Raimbault and Durrieu de Madron 2003) and exerts thereby a major ecological influence by enhancing primary productivity (Bosc et al. 2004).

In the Rhone River, export of annual suspended solid loads is concentrated during floods (Sempéré et al. 2000; Ollivier et al. 2011) with significant inputs from southern tributaries (Pont et al. 2002). For instance, the large flood that occurred in December 2003 exported 83 % of the total annual sediment load (Antonelli et al., 2008; Ollivier et al. 2010). As it covers a large drainage area (98,000 km^2) characterized by strong variations in climate and geological conditions, the relative contribution of the main Rhone River tributaries to its sediment discharge may vary throughout time (Pardé, 1925; Pont et al. 2002; Antonelli et al. 2008). Sediment conveyed by the Rhone River was documented to contain large concentrations in contaminants, such as organic pollutants (Sicre et al., 2008; Desmet et al. 2012; Mourier et al. 2014) and metals (Radakovitch et al. 2008). In addition, the Rhone valley represents Europe's largest concentration of nuclear power plants, and the river receives radioactive liquid effluents originating from four nuclear plants and a spent fuel reprocessing plant currently under dismantlement. As a consequence, sedimentary archives were shown to reflect significant enrichments in artificial radionuclides in the lower Rhone River sections (Ferrand et al. 2012). It is therefore crucial to better constrain those sources as marine sediments have the capacity to store these contaminants in continental shelf areas and in abyssal plains (Charmasson et al. 1998; Radakovitch et al. 1999; Lee et al. 2003; Garcia-Orellana et al. 2009).

In this context, quantifying the sources supplying sediments to the Rhone River and eventually to the Mediterranean Sea represents a crucial prerequisite for better understanding the riverine transfer and its potential role in global biogeochemical cycles, and for implementing effective control strategies to improve water and sediment quality (Walling and Collins 2008). The relative contribution of sediments originating from the main tributaries during the floods recorded in the lower sections of the Rhone River was shown to reflect lithological differences and to imprint the geochemical and mineralogical properties of the main upstream sediment sources (Pont et al. 2002; Ollivier et al. 2010; Zebracki et al. 2013a). We

therefore propose to use these sediment characteristics to fingerprint the origin of sediment transported in the lower Rhone River.

Exports of suspended sediments from the Rhone River have been continuously monitored since 2000 at the Rhone River Observatory Station in Arles (SORA), which is located 40 km upstream of its mouth. Furthermore, the suspended sediment content in natural and artificial radionuclides has been continuously analysed in the framework of legal radioecological surveillance (Eyrolle et al., 2012).

This study therefore proposes to provide alternative and original fingerprinting techniques based on radionuclide properties measured routinely to quantify the proportion of sediments supplied by the different tributaries to the Rhone River outlet during floods. Variations in geogenic ^{238}U, ^{232}Th and ^{40}K radionuclide activities may reflect the contribution of source areas with different lithologies (Olley et al. 1993; Yeager and Santschi 2003). In addition, among artificial radionuclides, spatial variations in ^{137}Cs and plutonium isotope activities (i.e., ^{238}Pu and $^{239+240}Pu$) may provide powerful tracers of the sediment origin. During Rhone River floods, ^{137}Cs was shown to originate mainly from erosion of the soils contaminated by global atmospheric fallout and Chernobyl accident (Antonelli et al. 2008), and to display an East-West decreasing gradient of contamination across the catchment (Renaud et al. 2003; Roussel-Debel et al. 2007). In contrast, and in the particular case of the lower Rhone River, Pu isotopes may either originate from erosion of the catchment soils contaminated by global atmospheric fallout or from remobilisation of sediment labeled by liquid effluents released by the Marcoule spent fuel reprocessing plant (from 1960s and decommissioned since 1997).
A method based on $^{238}Pu/^{239+240}Pu$ activity ratio (PuAR) measurements was developed to estimate the fraction of the Pu isotopes that originated from the Rhone River in marine deposits (Thomas 1997; Lansard et al. 2007). This method was applied to distinguish between Pu supply through soil erosion across the Rhone catchment and remobilisation of sediment stored in the river channel downstream of Marcoule, and to quantify their relative contribution to Pu fluxes recorded at Arles (Rolland 2006; Eyrolle et al. 2012).

After identifying the origin of floods, fingerprinting techniques presented above were applied to quantify the relative contribution of the main sources delivering sediments to the Rhone River, based on the continuous measurement of natural and artificial radionuclides. They were applied to suspended sediments collected at Arles outlet (SORA observatory station) between October 2000 and June 2012.

2 Study area

The Rhone River basin area consists of four mountainous subcatchments, i.e., Alps, Jura, Cevennes/Massif Central, and Vosges. In the northern part of the basin, the Jura and Vosges mountains (drained by the Saone River) are mainly calcareous. When moving to the South and to the East, the Alpine mountains (drained by the Upper Rhone, Isere and Durance rivers) mostly consist of sedimentary rocks and of siliceous crystalline and metamorphic rocks. Finally, in the southwestern part of the basin, crystalline siliceous rocks dominate in the Cevennes Mountains (drained by the Ardeche, Ceze and Gard rivers). Details on those geological substrate variations are given in Ollivier et al. 2010 and Ollivier et al. 2011. In addition to this geological heterogeneity, the Rhone basin is exposed to a wide variety of climate conditions (Pont et al. 2002). The tributaries of the Rhone are used to be organized in three main groups characterised by distinct hydrographic features (Figure 1): northern tributaries (Ain, Fier, Isere, Saone rivers) and southern tributaries, which may in turn be distinguished as Cevenol tributaries (Eyrieux, Ardeche, Ceze, Gard rivers) and southern Pre-Alpine tributaries (Durance, Drome, Aigues, and Ouveze rivers).

Forty kilometres upstream of its mouth the Rhone River subdivides into the Grand Rhone River and the Petit Rhone River, and flows into a delta of 1 500 km^2 (Figure 1). The sampling station in Arles is located on the Grand Rhone River, which drains about 90 % of the water discharge. The SORA observatory in Arles is an automatic sampling station operated by the French Institute for Radioprotection and Nuclear Safety (IRSN/LERCM).

At the Beaucaire gauging station (i.e., 8 km upstream of the Rhone difluence, and 14 km upstream of the SORA sampling station in Arles), the Rhone mean annual discharge was about 1,700 $m^3.s^{-1}$ for the period 1920-2012, while the annual suspended solid load varied from 1.2 to 19.7 $Mt.yr^{-1}$ for the period 1961-1996 (Antonelli 2002; Pont et al. 2002). River discharges associated with the 1-yr, 2-yr,

10-yr, and 100-yr return periods amount to 4,000, 5,000, 8,400 and 11,200 $m^3.s^{-1}$, respectively.

3 Materials and methods

3.1 Flood classification

Based on the previous description of the flood types (Parde 1925), four types of climatological regimes are distinguished (Figure 1):

(1) Oceanic floods generally occurring in winter and resulting from rainfall in the northern part of the basin (Fier, Ain, Isere, Saone rivers);

(2) Cevenol floods occurring mainly in autumn and resulting from flash-flood type storms affecting the southwestern tributaries of the Rhone River (Ardeche, Ceze, Gard, Eyrieux rivers);

(3) Extensive Mediterranean floods resulting from precipitations affecting the right bank area of the river (Cevenol tributaries listed above) and the sub-Alpine tributaries located on the left bank of the Rhone River (Durance, Ouveze West Bank, Aigues rivers as well as to a lesser extent the Drome River);

(4) Generalized floods mostly occurring in autumn and affecting both northern and southern tributaries.

During the period 2000-2012, water discharge data recorded at Arles gauging station and downstream of the twelve tributaries mentioned above were provided by the *Compagnie Nationale du Rhône* (CNR).

Flood classification was performed by comparing the rise in water discharge registered at the Rhone River monitoring station during sampling to the hydrographs of the relevant upstream tributaries (according to the method described by Pont et al. 2002, Rolland 2006, and Antonelli et al. 2008).

Flood classification was refined by considering the mean maximal daily water discharge recorded during floods (Zebracki et al. 2013b) to discriminate between small-scale floods (3,000–4,000 $m^3.s^{-1}$), intermediate floods (4,000–5,000 $m^3.s^{-1}$), large-scale floods (5,000–9,000 $m^3.s^{-1}$), and exceptional floods (> 9,000 $m^3.s^{-1}$).

3.2 Suspended sediment sampling procedures during flood events

3.2.1 Particle-associated radionuclides

Sampling procedures during periods of high water discharge (> 3,000 $m^3.s^{-1}$) are detailed in Eyrolle et al. 2012. Briefly, since 2005, 5 L water samples were

collected every 20 minutes and directly filtered onto 0.5 µm Milligard® cellulose acetate cartridges. The filter clogging was continuously monitored, so that the filtration was stopped when 50 % of clogging was achieved or after 8 hours. Subsequent water samples were then collected on successive filters, which were analysed separately. Before 2005, samples were manually collected during floods.

Additional suspended sediment samples were obtained either after filtering river water through Milligard® cartridges or by decanting suspended matter contained in at least 120 L river water samples.

3.2.2 Suspended sediment load

Sampling procedures during periods of high water discharge (> 3,000 $m^3.s^{-1}$) are detailed in Eyrolle et al. 2012. In summary, six suspended sediment samples were collected daily to improve flood monitoring by collecting 150 mL every 30 min. Before 2005, samples consisted of manual collection of river water at hourly time step.

The suspended sediment load exported during floods was calculated from river discharge and suspended sediment concentration records.

3.3 Radionuclide analyses on suspended sediment collected at Arles station

3.3.1 Gamma emitters

For gamma spectrometry analyses suspended sediment samples were ashed and put into tightly closed plastic boxes for gamma counting (20-60 g) using low-background and high resolution Germanium Hyper pure detectors at the IRSN/LMRE laboratory in Orsay (Bouisset and Calmet 1997). For each sample, up to 29 gamma-emitting radionuclides (both natural and artificial) were determined. Time between sampling and analysis varied between 29 and 333 days, with a mean of 77 d.

In this study, we restricted the analysis to measurements of ^{40}K, ^{232}Th, ^{238}U (natural radionuclides) and ^{137}Cs (artificial radionuclide). Due to their long-term radioactive decay, the activities in ^{232}Th and ^{238}U were estimated by measuring the contents of their short-lived filiation products, i.e., ^{228}Ac and ^{234}Th respectively, and assuming secular equilibrium within the corresponding radioactive decay series. The use of ^{228}Ac as a proxy to estimate ^{232}Th content in sediment relies on the assumption that ^{228}Ra is not preferentially remobilised in the riverine system.

Efficiency calibrations were constructed using gamma-ray sources in a 1.15 $g.cm^{-3}$ density solid resin-water equivalent matrix. Activity results were corrected for true

coincidence summing and self-absorption effects (Lefèvre et al. 2003). Measured activities, expressed in $Bq.kg^{-1}$ dry weight, are decay-corrected to the date of sampling. The activity uncertainty was estimated as the combination of calibration uncertainties, counting statistics, and summing and self-absorption correction uncertainties.

3.3.2 Alpha emitters

When available sample amount was sufficient (i.e., 50-200 g of dry matter), analyses of plutonium isotopes (^{238}Pu and $^{239+240}Pu$) were performed by alpha spectrometry at IRSN/LMRE (Goutelard et al. 1998; Lansard et al. 2007). In brief, ashed samples were leached with nitric acid, co-precipitated and purified using exchange resins before electro-deposition, and then counted on low background PIPS® detectors for up to 14 days. The detection limit for the analytical procedure was 1 mBq for both ^{238}Pu and $^{239+240}Pu$.

3.4 Sediment sources natural radionuclides ^{238}U, ^{232}Th and ^{40}K contents

Based on the signatures of different lithological sources previously described for the Rhone River basin (Pont et al., 2002; Ollivier et al., 2010), we identified three main contrasting source areas, i.e., “Upstream”, “Pre-Alpine”, and “Cevenol” sediment sources, corresponding to (1) the northern part of the Rhone basin (mainly calcareous), (2) the southern-left bank of the river (sedimentary rocks), and (3) the southern-right bank area (crystalline siliceous rocks).

Natural radionuclide contents in these three sediment sources were assessed based on a set of available fine-grained sediment samples (Figure 1). Radionuclide composition of the southern-right bank source was measured in suspended material transported during flood events recorded on the Ardeche, Ceze and Gard Rivers in December 2003 (Rolland 2006), November 2011 and November 2012. Radionuclide composition of the southern-left bank originating sediment was measured on the sediment core layers that were estimated to have deposited between 2000 and 2009 at the outlet of the Bleone River, i.e., the main tributary of the Durance River (Navratil et al., 2012. Radionuclide properties of the third sediment source area, i.e., the upstream tributaries flowing into the Rhone River upstream of the Cevenol tributaries, were assessed by using a sediment core collected in 2011 in the so-called “Grange Ecrasee” secondary channel of the Rhone River, ca. 15 km upstream of its confluence with the southern tributaries (Mourier et al. 2014). Sediment core

layers were collected in low water flow conditions that allowed for sediment deposition. The collected sediment was characterised by the dominance of silt- and clay-sized material (i.e. < 63 µm; 80 % of material in the Bleone River core, and 73 % in the Grange Ecrasee core). Unfortunately, grain size composition of suspended sediment collected in the framework of continuous radiological monitoring was not measured routinely, but available measurements show that this material is fine-grained and that the clay and silt fractions are dominant (Antonelli et al. 2008). Direct comparison of radionuclide activities measured in both subcatchment source material and in riverine suspended sediment was therefore considered to be relevant and meaningful (e.g., Navratil et al. 2012).

3.5 Fingerprinting the sources delivering suspended sediment to the Lower Rhone River

3.5.1 Based on natural radionuclides ^{238}U, ^{232}Th and ^{40}K

The natural radionuclide composition in ^{238}U, ^{232}Th and ^{40}K of the three sediment sources (i.e., Upstream, Cevenol, Pre-Alpine) was assessed based on radionuclide measurements in sediments representative of each subcatchment source. The ability of these geogenic fingerprints to discriminate between the potential sediment sources was assessed by conducting a range test (i.e., radionuclide activities of suspended sediments discharged at the outlet of the Rhone River were comprised in the range of values defined by those of the three sediment sources), and by a non-parametric Kruskal–Wallis *H*-test (Collins and Walling 2002). The set of the three geogenic radionuclides ^{238}U, ^{232}Th and ^{40}K successfully passed the Kruskal–Wallis *H*-test. By performing a stepwise selection procedure, the combination of the three geogenic radionuclides provided a good discrimination of the different sources as they were associated with low Wilk's lambda values. A multivariate mixing model was then used to estimate the relative contribution of the potential sediment sources in each outlet sediment sample. By assuming a normal distribution for each fingerprinting property and source, a series of 10,000 random positive numbers was generated from these distributions and used to estimate the relative contribution of the potential sources in the sediment samples. The robustness of the source ascription solutions were assessed using a mean "goodness of fit" (GOF) index (Motha et al. 2003). Only the sets of simulated random numbers that obtained a GOF index value higher than 0.80 were used in the subsequent steps. The use of the Monte Carlo method allowed the calculation

of 95 % confidence intervals. The outputs of the mixing model appeared to be very stable, all outputs being very close (and systematically within a range of ± 2 %) to their mean value. It was therefore decided to present only those mean values in the remainder of the text.

A detailed description of these procedures is provided in Evrard et al. (2011) and Haddadchi et al. (2013).

3.5.2 Based on artificial radionuclides ^{137}Cs, ^{238}Pu and $^{239+240}Pu$

3.5.2.1 $^{238}Pu/^{239+240}Pu$ Activity ratio (Pu AR)

From analyses performed on French riverine sediments collected between 2003 and 2005, the $^{238}Pu/^{239+240}Pu$ activity ratio (Pu AR) characterizing the global atmospheric fallout was estimated to 0.036±0.006 (Eyrolle et al. 2008), whereas the Marcoule radioactive liquid releases are characterized by a theoretical constant Pu AR of 0.3 (Lansard et al. 2007). Within the river section located downstream of Marcoule and assuming that no direct release of Pu occurs when water discharge exceeds 4,000 $m^3.s^{-1}$ (Rolland 2006), Pu isotope contents in suspended sediment result from the mixed contribution of erosion of soils of the Rhone catchment and remobilisation of sediment deposits labeled by the Marcoule radioactive releases. At the monitoring station in Arles, based on activity measurements in ^{238}Pu and ^{239}Pu of suspended sediment, samples display Pu AR values corresponding to the mixing of both sources (Eq. 2):

$$\frac{^{238}Pu_{Sample}}{^{239+240}Pu_{Sample}} = \frac{^{238}Pu_{Marcoule} + ^{238}Pu_{Catchment}}{^{239+240}Pu_{Marcoule} + ^{239+240}Pu_{Catchment}} \quad (2)$$

The fractions of the total Pu isotopes that were discharged at Arles and the ones that were derived from sediment remobilisation ($^{238}Pu_{Sed}$ and $^{239+240}Pu_{Sed}$, in percentage) are quantified using the following relationships (Eq. 3 and 4):

$$^{239+240}Pu_{Sed} = \frac{PuAR_{Sample} - PuAR_{Catchment}}{PuAR_{Marcoule} - PuAR_{Catchment}} \times 100 \quad (3)$$

$$^{238}Pu_{Sed} = ^{239+240}Pu_{Sed} \times \frac{PuAR_{Marcoule}}{PuAR_{Sample}} \quad (4)$$

The uncertainty associated with each contribution was constrained by the standard analytical deviation.

3.5.2.2 $^{137}Cs/^{239+240}Pu$ Activity ratio (Cs/Pu AR)

3.5.2.2.1 Cs/Pu AR in soils of the Rhone basin

The ^{137}Cs contained in soils of the Rhone catchment originates from both the global atmospheric fallout (nuclear weapons testing from 1945 to the beginning of 1980s) and Chernobyl accident (1986). In contrast $^{239+240}Pu$ in the soils of the Rhone catchment was exclusively supplied by the global atmospheric fallout as no additional plutonium supply was detected in the environment in France after Chernobyl accident (Renaud et al. 2007).

Total theoretical atmospheric deposition of ^{137}Cs on soils was previously mapped at the scale of France by using two empirical relationships (Roussel-Debet et al. 2007): the first one linking the mean annual amount of rainfall and the cumulative deposition from 1945 to 1982 for fallout supplied by the atmospheric nuclear weapon tests (Mitchell et al. 1990), and the second one associating the activity levels measured in soils with the daily rainfall recorded just after Chernobyl accident (Renaud et al. 2003).

Based on the $^{137}Cs/^{239+240}Pu$ activity ratio characteristic of the global atmospheric fallout (e.g., Masson et al. 2010), and the available cartography of ^{137}Cs deposition (Roussel-Debet et al. 2007), the spatial distribution of $^{137}Cs/^{239+240}Pu$ activity ratio (Cs/Pu AR) was mapped at the scale of the Rhone basin and decay-corrected to 1/1/2010.

Although radiocaesium and plutonium are chemically dissimilar elements, it has been shown that ^{137}Cs and $^{239+240}Pu$ originating from atmospheric fallout remained fixed together in soils over decades, suggesting the absence of geochemical fractionation (Hodge et al. 1996).

Based on values found in the literature, the theoretical Cs/Pu AR in the Rhone basin was decay-corrected in order to match with the study period (2000-2012) and displayed values within the range of 27-42 (Hodge et al. 1996; Cochran et al. 2000; Le Roux et al. 2010).

The mean Cs/Pu AR was then calculated for each subcatchment of the Rhone basin. Deviation in this theoretical Cs/Pu AR indicates the supply of additional radionuclide contamination by other sources than the bomb fallout (Hodge et al. 1996; Turner et al. 2003; Antovic et al. 2012). In the Rhone basin, this additional source originates from the Chernobyl fallout.

3.5.2.2.2 Cs/Pu AR in suspended sediments of the lower Rhone River

In suspended sediment exported at the outlet of Rhone River, ^{137}Cs and $^{239+240}Pu$ originate from two sources: the erosion of Rhone catchment soils and the liquid radioactive releases from nuclear industries (the Marcoule spent fuel reprocessing plant for $^{239+240}Pu$ and ^{137}Cs, and nuclear power plants for ^{137}Cs).
The contribution from waste facilities originates either from direct releases or from sediment remobilisation processes. Releases from nuclear industries are submitted to authorisation and liquid discharges are not allowed during periods of high water discharge (threshold of 4,000 $m^3.s^{-1}$ at Arles gauging station [Rolland 2006]).

Contrary to $^{238}Pu/^{239+240}Pu$, no specific signature in $^{137}Cs/^{239+240}Pu$ of radioactive liquid releases has been identified so far. Among the nuclear facilities, the potential source of Pu is unique (Marcoule reprocessing plant), whereas there are potentially various sources of ^{137}Cs. Based on annual data chronicles of ^{137}Cs and $^{239+240}Pu$ released in the Rhone River between 1963 and 2003 (Eyrolle et al. 2005), the Cs/Pu AR was assessed in order to characterise the Marcoule reprocessing plant signature.

The $^{137}Cs/^{239+240}Pu$ activity ratio in sediments may be affected by the different geochemical behaviour of both elements and by their various sediment-water distribution coefficients (K_d). However, it was shown that both artificial radionuclides were strongly fixed to particles in freshwater environments (Cochran et al. 2000; Le Cloarec et al. 2007). Our interpretations of the Cs/Pu AR variations therefore relied on the hypothesis that both elements displayed a similar behaviour in this environment and that they were strongly particle-reactive.

The uncertainty associated with $^{137}Cs/^{239+240}Pu$ values was calculated based on the standard analytical deviation.

3.5.3 Coupling artificial and natural radionuclides methods

The three potential sediment sources that were discriminated by the fingerprinting method based on natural radionuclides were also characterised by their Cs/Pu AR. By coupling the Cs/Pu AR characteristics to the relative contribution of sediment sources that resulted from the fingerprinting method based on natural radionuclides, we calculated the expected values of Cs/Pu AR (Cs/Pu AR exp) and

compared them to the calculated values of Cs/Pu AR resulting from radionuclide measurements in suspended sediments (Cs/Pu AR SS).

4 Results and discussion

4.1 Sample collection and flood classification

Between October 2000 and June 2012, 221 samples were collected during floods at Arles. Those suspended sediment samples were taken during 37 flood events and document 85 % of the floods that were recorded at Arles station during this period (Supplementary information Figure S1). During this study, floods were dominated by the occurrence of small-scale floods (76 %), followed in decreasing importance order by intermediate floods (11 %), large floods (8 %) and exceptional floods (5 %) corresponding to two flood events that occurred during autumn in 2002 and during winter in 2003.

All floods that occurred in the lower section of the Rhone River could be classified according to the proposed scheme (Table 1) with the exception of two floods that occurred in 2010 (September and March). Both floods were characterised by a relatively low maximum 1-h water discharge (< 3,100 $m^3.s^{-1}$) with no clear evolution throughout time. However, the number of suspended sediment samples collected during both floods (*i.e.*< 3 % of the total) is negligible compared to the entire dataset available. Unclassified suspended sediment samples were therefore removed from further analysis.

Generalised, Oceanic, Cevenol and extensive Mediterranean floods were documented by 40, 23, 23 and 11 % of the samples, respectively. All the flood types were well represented in the compiled database. This database is therefore representative of the entire range of flood types that occurred during the last decade.

4.2 Fingerprinting based on natural radionuclides

4.2.1 Activities in ^{238}U, ^{232}Th, ^{40}K and sediment source characteristics

Activities in ^{238}U, ^{232}Th and ^{40}K of suspended sediment collected in the lower Rhone River show that they were influenced by the flood type (Figure 2). When comparing ^{238}U, ^{232}Th and ^{40}K activities in suspended sediment according to the flood type, Cevenol events displayed the highest median values of all parameters suggesting a specific signature of southwestern tributaries (Figure 2).

Cevenol floods display a geogenic radionuclide signature distinct from the other floods. This difference could not only be due to specific lithological characteristics but also to preferential conditions of sediment transport, as these floods display typical flash-flood characteristics and their source area is located at a shorter distance from the outlet sampling station.

The difference observed in ^{238}U, ^{232}Th and ^{40}K activities among the three sediment sources provided a sound physico-chemical basis to discriminate between their respective contributions at the Rhone River basin scale (Table 2, Supplementary information Tables S1, S2 and S3). As expected, the Cevenol granitic sediment source displayed the most enriched composition in all three natural radionuclides, whereas their activities were the lowest in calcareous Pre-Alpine sources. The larger variations associated with parameters characterising the Cevenol source can be attributed to the larger spatial heterogeneity of this potential sediment source.

4.2.2 Sediment source contribution

The contribution of each sediment source, i.e., Upstream, Cevenol and Pre-Alpine, to suspended sediment conveyed during floods in the Lower Rhone River is displayed in Figure 3.

Cevenol floods were characterised by the highest interquartile range (i.e. difference between the third and first quartiles; Figure 3b), reflecting the highest temporal variability of sediment supply during these typical “flash-flood” events. The mean contribution of sediment from Upstream, Pre-Alpine and Cevenol sources amounted to 31 %, 30 % and 39 % of the total sediment input to the outlet, respectively (Figure 3b). Although Cevenol floods were of relatively short duration (from a few hours to a few days), they supplied an equivalent amount of sediment as the two other sources to the outlet at a decadal timescale.

During extensive Mediterranean, Oceanic and generalised floods (Figure 3acd), Pre-Alpine and Upstream inputs supplied a mean of 38-53 % and 36-39 % of the total Rhone sediment export, and were therefore the main sediment contributors.

When comparing Oceanic floods with other flood types (Figure 3), we may have expected a significantly larger contribution of Upstream sediment. However, this was not observed, suggesting that material eroded in the northern part of the catchment may not reach the outlet (at Arles) rapidly enough to imprint its

signature on material conveyed downstream. Contrary to Cevenol floods, Oceanic floods are characterised by a slow and regular rise in water discharge. Those specific sediment transport conditions combined with the presence of numerous dams in this upper catchment part likely resulted in the significant storage of material in reservoirs (Pont et al. 2002; Ollivier et al. 2010).

4.2.3 Sediment load contribution

Suspended sediment load was determined for all floods documented between 2000 and 2012, with the exception of 4 events (Nov. 2000, March and April 2001, and Nov. 2004) for which the number of samples was considered not to be sufficient, or because of the lack of precision in the timing of sample collection. Fourteen samples (6 % of the entire sample set) were associated with those floods and were therefore removed from further analysis.

By summing individual sediment loads associated with successive samples, the total amount of suspended sediment discharged during floods between 2000 and 2012 was estimated to 19.5×10^6 tons. This amount is underestimated as 30 % of flood events could not be sampled or were not completely documented by the monitoring. Furthermore, it should be reminded that the precision of solid flux estimations is strongly dependent on the sampling of suspended sediment concentration variations during the floods (Ollivier et al. 2010). The sediment flux during floods could not be compared with the total sediment export to the sea during the entire study period, as corresponding data were not available for low water flow periods. A rough comparison with previous findings outlines the strong variability of both inter- and intra-annual fluxes of sediment in the Rhone River (Supplementary information Table S4).

The contribution of suspended sediment originating from each source is represented in Figure 4a. The sediment supply from Pre-Alpine, Upstream, and Cevenol sources was estimated to 10, 6.8 and 2.2×10^6 tons, respectively. The sediment inputs from southern tributaries (i.e., Pre-Alpine and Cevenol) accounted for 65 % of the total particulate flux, which is close to the results reported by Pont et al. 2002 (i.e., 72 %, Supplementary information Table S4). Our results further highlight the dominant role of Pre-Alpine tributaries (and especially the Durance River) as the main sediment supply (53 %) to the Rhone during floods.

During generalised, extensive Mediterranean, Cevenol and Oceanic floods, sediment export was estimated to 11, 6.4, 1.4 and 0.7×10^6 tons of sediment, respectively (Figure 4b). Generalised and extensive Mediterranean floods thereby deliver the bulk of the Rhone sediment to the sea (87 % of the total sediment supply).

4.3 Fingerprinting based on artificial radionuclides

4.3.1 Activity ratio $^{238}Pu/^{239+240}Pu$

During floods, the calculated Pu AR activity ratio exceeded systematically the reference value in the catchment soils (i.e., 0.036±0.006, see Table 3). This reflects the continuous occurrence of remobilisation of Marcoule-labeled sediment and confirms that sediment remobilisation provides a significant secondary source of Pu to the Rhone River prodelta (Miralles et al. 2004; Eyrolle et al. 2006; Lansard et al. 2007) and the offshore zone (Garcia-Orellana et al. 2009; Dufois et al. 2014).

At a given date, the contribution of ^{238}Pu originating from remobilised sediment was systematically higher than the $^{239+240}Pu$ fraction (Table 3). In most cases, sediment remobilisation was shown to act as the primary source of ^{238}Pu in suspended sediment discharged by the Rhone River, whereas soil erosion in the Rhone catchment provided the dominant source of $^{239+240}Pu$. The enrichment of sediment in ^{238}Pu compared to $^{239+240}Pu$ is therefore a consequence of mixing between sediment labeled by nuclear effluent releases into the Rhone River and erosion of soil material from the catchment (Eyrolle et al. 2004).

The highest contribution of Pu-labeled sediment remobilisation occurred during floods characterised by the highest water discharges (82-88 % for ^{238}Pu and 36-47 % for $^{239+240}Pu$ on 11/26/2002, 12/02/2003 and 12/03/2003, Table 3). The contribution of remobilised sediment is controlled by specific physical properties of sediment during reworking processes, such as critical shear stress (Lau and Droppo 2000; Gerbersdorf et al. 2007), which can be enhanced with increasing water discharge.

However, high contributions (> 70 % for ^{238}Pu) of Pu-labeled remobilised sediment were also recorded during intermediate floods, suggesting that water discharge is not the single factor controlling sediment remobilisation. The proportion of Pu derived from the remobilisation of sediment is also controlled by the flush of

temporarily stored sediment and the heterogeneous labelling of sediment by Pu (Eyrolle et al. 2012).

At a given discharge, the fraction of remobilised sediment enriched in Pu displays a large inter- and intra-flood variability, suggesting the lack of control achieved by the suspended sediment origin and the flood type (Table 3). For example, at discharges comprised between 4,000 and 4,100 $m^3.s^{-1}$, the fraction of remobilised sediment varies by a factor of 2 between two Cevenol floods in November 2008 and 2011. At ~5,300 $m^3.s^{-1}$, the remobilised sediment fraction varies by a similar factor between generalised and Cevenol floods that occurred in November 2002 and 2008. The fractions of Pu-labeled remobilised sediment reached minimum values during the flood of May 2008 (4–5 % for ^{238}Pu, Table 3), indicating an unusual supply of Pu-depleted sediment that was attributed to simultaneous dam releases that occurred upstream of Marcoule reprocessing plant and that likely supplied material depleted in plutonium (Eyrolle et al. 2012).

Although sediment reworking occurs routinely and a substantial decrease of Marcoule plutonium releases was documented after 1997 (Eyrolle et al. 2005), we could not observe any significant decreasing trend in Pu AR evolution between 2000 and 2011, suggesting that the stock of Pu-labeled sediment may not have decreased significantly at a decadal timescale or that Pu releases continued significantly after 1997.

4.3.2 Activity ratio $^{137}Cs/^{239+240}Pu$

4.3.2.1 In soils

The spatial distribution of $^{137}Cs/^{239+240}Pu$ activity ratio in soils estimated based on the theoretical deposition of both radionuclides is heterogeneous across the Rhone River basin (Figure 5).

The mean Cs/Pu AR estimated for each subcatchment was systematically higher than the ratio characteristic of global atmospheric fallout (i.e., 27-42), reflecting the additional supply of ^{137}Cs from Chernobyl accident (Table 4). In the southern part of the Rhone basin (Figure 5, Table 4), the East-West decreasing gradient of this ratio clearly indicates that soils drained by Pre-Alpine tributaries (Durance, Aigues, Ouveze, Drome rivers) were more contaminated by Chernobyl ^{137}Cs fallout

(Cs/Pu AR between 108-136) than those drained by Cevenol tributaries (Ardeche, Gard, Ceze river; Cs/Pu AR between 47-56).

4.3.2.2 In suspended sediments

Activities in ^{137}Cs of suspended sediments varied between 3.0±0.4 and 35±3 $Bq.kg^{-1}$ (Supplementary information Table S5). This variability may reflect the difference in sediment origin, as it was shown that grain size did not significantly influence activities in ^{137}Cs of suspended sediment transported during floods at this station (Antonelli et al. 2008). The mean ^{137}Cs activity for the period 2001-2012 was estimated to 10±5 $Bq.kg^{-1}$, which is lower although not significantly different from annual records documenting the "anthropogenic background" of the Rhone basin (i.e., 14.9±0.4 $Bq.kg^{-1}$ reported by Antonelli et al. 2008, and 15±4 $Bq.kg^{-1}$ reported by Eyrolle et al. 2012).

Contrary to $^{238}Pu/^{239+240}Pu$, a specific $^{137}Cs/^{239+240}Pu$ activity ratio could not be attributed to radioactive liquid releases of Marcoule reprocessing plant. Estimations vary between 24 and 3,727, and this range of values is too broad for quantifying the specific contribution of these radioactive releases to suspended sediment.

When plotting $^{239+240}Pu$ vs. ^{137}Cs activities in suspended sediment collected during floods, the obtained positive relationship confirms the contribution of a single source (i.e., erosion of Rhone catchment soils) supplying both radionuclides to the lower Rhone River (Figure 6, data are given in Supplementary information Table S5), and that the contribution of $^{239+240}Pu$ originating from the remobilisation of sediment downstream of Marcoule may be considered to be of minor importance compared to catchment contribution (Table 3).

Cs/Pu ARs measured in suspended sediment were systematically higher than the characteristic global atmospheric fallout ratio (i.e., 27-42), reflecting the additional input of ^{137}Cs from the Chernobyl fallout (Supplementary information Table S5).

Although $^{239+240}$Pu and ^{137}Cs activities in suspended sediment conveyed during floods are correlated (Figure 6), the mean ^{137}Cs/$^{239+240}$Pu activity ratio slightly differed for the different flood types. As expected from the mapping of Cs/Pu AR in the southern part of the Rhone basin, suspended sediment that originated from Cevenol tributaries displayed the mean lowest Cs/Pu AR (i.e., 54 ± 6) whereas suspended sediment supplied by Pre-Alpine tributaries displayed the mean highest Cs/Pu AR (i.e., 78 ± 10). Sediment exported during generalised floods showed a higher variability in Cs/Pu AR due to the mix of the various potential sediment sources at the entire Rhone basin scale (mean Cs/Pu AR equal to 71 ± 16). No specific signature was expected in suspended sediment exported during Oceanic floods (mean Cs/Pu AR equal to 70 ± 17), since Upstream sediment source was characterised by intermediary Cs/Pu AR values comprised between the signatures of Cevenol and Pre-Alpine sediment sources.

4.3.3 Expected and calculated Cs/Pu AR in suspended sediment

Based on the theoretical value of ^{137}Cs/$^{239+240}$Pu activity ratio in soils of the different subcatchments (Table 4), each potential sediment source was characterised by its mean Cs/Pu AR: 132 ± 19, 73 ± 22 and 51 ± 5 for Pre-Alpine, Upstream and Cevenol sources, respectively. By combining artificial radionuclide characteristics for these three sediment sources and the contribution of each sediment source (in percentage) obtained by the fingerprinting method based on natural radionuclides (see 3.2.2), the expected Cs/Pu AR were estimated in suspended sediment (Supplementary information Table S5).

All Cs/Pu AR calculated from artificial radionuclide measurements conducted on suspended sediment (Cs/Pu AR SS) were comprised in the range of variation of expected Cs/Pu AR (Cs/Pu AR exp). Although values were not significantly different, the discrepancy between expected and calculated Cs/Pu AR generally indicated an underestimation of expected values. This observation may be due to the strong dilution of the initial signature of Cs/Pu AR in soils because of the occurrence of physical and dynamical processes such as erosion, deposition and reworking processes during the decades that followed the last ^{137}Cs inputs in 1986. Alternatively, this underestimation could be due to contribution of sediment depleted in artificial radionuclides and supplied by subsurface erosion such as riverbanks or deep gullies (Ben Slimane et al. 2013; Evrard et al. 2013).

5 Conclusions

This study provided to our knowledge the first attempt to combine the use of a continuous river monitoring network and sediment fingerprinting based on natural and artificial radionuclides to quantify the respective contribution of subcatchments to sediment transported during floods at the outlet of a large river basin (98,000 km^2).

A first fingerprinting method based on measurements of natural radionuclides (^{238}U, ^{232}Th and ^{40}K) allowed the quantification of the relative contribution of each potential sediment source. The total amount of suspended sediment exported during floods for the period 2000-2012 was estimated to $19.5x10^6$ tons. Pre-Alpine, Upstream, and Cevenol sources contributed to 53, 35 and 11 % of the total sediment supply, respectively. Pre-Alpine tributaries were thereby shown to be the main sediment supplier to the lower Rhone River during floods. Then, the results provided by an alternative method based on artificial radionuclide measurements ($^{137}Cs/^{239+240}Pu$ activity ratio) failed to achieve this objective at the basin scale, because of the heterogeneous spatial pattern of ^{137}Cs deposition after Chernobyl accident that did not coincide with the delineation of the above-mentioned subcatchment sources. However, it provided a relevant discrimination between the respective contributions of western and eastern tributaries in the southern part of the Rhone basin.

In addition, the method based on $^{238}Pu/^{239+240}Pu$ activity ratio demonstrated the continuous remobilisation of local Pu-labeled sediment and showed that the stock of Pu-contaminated sediment in the Lower Rhone River may not have decreased significantly during the decade that followed the dismantlement of the spent fuel reprocessing plant. These natural and artificial radionuclide activities may then further be used to better understand the fate of sediment supplied to the Mediterranean Sea.

In future, fingerprinting based on natural radionuclides could usefully be applied to catchments characterized by lithological variations. Furthermore, methods based on artificial radionuclides measurements ($^{137}Cs/^{239+240}Pu$ activity ratio) may be applied to catchments characterised by spatial heterogeneous patterns of ^{137}Cs deposition.

Acknowledgements

This work was supported by the Rhone Sediment Observatory (OSR) from ZABR and by AERMC (Agence de l'Eau Rhône-Méditerranée-Corse). Liquid discharge data in the Rhone River and its tributaries were available from the CNR (Compagnie Nationale du Rhône, http://www.cnr.tm.fr/fr/). Daily suspended sediment load data were provided by Patrick Raimbault (MIO) from MOOSE/SOERE.

The authors gratefully acknowledge Vincent Boullier, Benoît Rolland and IRSN/LERCM team, Marc Desmet (GEHCO), Jean Philippe Bedell (ENTPE), and Michel Fornier (MIO) for their help during field and laboratory works, and IRSN/LMRE team and Irène Lefèvre (LSCE) for sample analyses.

The authors also gratefully thank the five anonymous reviewers whose suggestions greatly improved the quality of the manuscript.

Appendix A. Supplementary data

Supplementary data associated with this article can be found in the online version.

References

Antonelli, C., 2002. Flux sédimentaires et morphogenèse récente dans le chenal du Rhône aval. Ph.D. thesis, University of Aix-Marseille I., France, 272 pp.

Antonelli, C., F. Eyrolle, B. Rolland, M. Provansal and F. Sabatier (2008). "Suspended sediment and ^{137}Cs fluxes during the exceptional December 2003 flood in the Rhone River, southeast France." Geomorphology **95**(3-4): 350-360.

Antovic, N. M., P. Vukotic, N. Svrkota, S. K. Andrukhovich (2012). "Pu-239+240 and Cs-137 in Montenegro soil: their correlation and origin." Journal of Environmental Radioactivity **110**: 90-97.

Ben Slimane, A., D. Raclot, O. Evrard, M. Sanaa, I. Lefèvre, M. Ahmadi, M. Tounsi, C. Rumpel, A. Ben Mammou, Y. Le Bissonnais (2013). "Fingerprinting sediment sources in the outlet reservoir of a hilly cultivated catchment of Tunisia." Journal of Soils and Sediments **13**(4): 801-815.

Bosc, E., A. Bricaud and D. Antoine (2004). "Seasonal and interannual variability in algal biomass and primary production in the Mediterranean Sea, as derived from 4 years of SeaWiFS observations." Global Biogeochemical Cycles **18**(1): GB1005.

Charmasson, S., O. Radakovitch, M. Arnaud, P. Bouisset, A.-S. Pruchon (1998). "Long-core profiles of ^{137}Cs, ^{134}Cs, ^{60}Co and ^{210}Pb in sediment near the Rhône River (Northwestern Mediterranean Sea)." Estuaries **21**(3): 367-378.

Cochran, J. K., S. B. Moran, N. S. Fisher, T. M. Beasley and J. M. Kelley (2000). "Sources and transport of anthropogenic radionuclides in the Ob River system, Siberia." Earth and Planetary Science Letters **179**(1): 125-137.

Collins, A. L. and D. E. Walling (2002). "Selecting fingerprint properties for discriminating potential suspended sediment sources in river basins." Journal of Hydrology **261**(1–4): 218-244.

Delmas, M., O. Cerdan, B. Cheviron, J.-M. Mouchel, F. Eyrolle (2012). "Sediment export from French rivers to the sea." Earth Surface Processes and Landforms **37**(7): 754–762.

Desmet, M., B. Mourier, B. J. Mahler, P. C. Van Metre, G. Roux, H. Persat, I. Lefèvre, A. Peretti, E. Chapron, A. Simonneau, C. Miège and M. Babut (2012). "Spatial and temporal trends in PCBs in sediment along the lower Rhône River, France." Science of the Total Environment **433**(0): 189-197.

Dufois, F., R. Verney, P. Le Hir, F. Dumas and S. Charmasson (2014) "Impact of winter storms on sediment erosion in the Rhone River prodelta and fate of sediment in the Gulf of Lions (North Western Mediterranean Sea)." Continental Shelf Research **72**: 57-72.

Durrieu de Madron, X., C. Guieu, R. Sempéré, P. Conan, D. Cossa, F. D'Ortenzio, C. Estournel, F. Gazeau, C. Rabouille, L. Stemmann, S. Bonnet, F. Diaz, P. Koubbi, O. Radakovitch, M. Babin, M. Baklouti, C. Bancon-Montigny, S. Belviso, N. Bensoussan, B. Bonsang, I. Bouloubassi, C. Brunet, J. F. Cadiou, F. Carlotti, M. Chami, S. Charmasson, B. Charrière, J. Dachs, D. Doxaran, J. C. Dutay, F. Elbaz-Poulichet, M. Eléaume, F. Eyrolles, C. Fernandez, S. Fowler, P. Francour, J. C. Gaertner, R. Galzin, S. Gasparini, J. F. Ghiglione, J. L. Gonzalez, C. Goyet, L. Guidi, K. Guizien, L. E. Heimbürger, S. H. M. Jacquet, W. H. Jeffrey, F. Joux, P. Le Hir, K. Leblanc, D. Lefèvre, C. Lejeusne, R. Lemé, M. D. Loÿe-Pilot, M. Mallet, L. Méjanelle, F. Mélin, C. Mellon, B. Mérigot, P. L. Merle, C. Migon, W. L. Miller, L. Mortier, B. Mostajir, L. Mousseau, T. Moutin, J. Para, T. Pérez, A. Petrenko, J. C. Poggiale, L. Prieur, M. Pujo-Pay, V. Pulido, P. Raimbault, A. P. Rees, C. Ridame, J. F. Rontani, D. Ruiz Pino, M. A. Sicre, V. Taillandier, C. Tamburini, T. Tanaka, I. Taupier-Letage, M. Tedetti, P. Testor, H. Thébault, B. Thouvenin, F. Touratier, J. Tronczynski, C. Ulses, F. Van Wambeke, V. Vantrepotte, S. Vaz and R. Verney (2011). "Marine ecosystems' responses to climatic and anthropogenic forcings in the Mediterranean." Progress in Oceanography **91**(2): 97-166.

Evrard, O., O. Navratil, S. Ayrault, M. Ahmadi, J. Némery, C. Legout, I. Lefèvre, A. Poirel, P. Bonté and M. Esteves (2011). "Combining suspended sediment monitoring and fingerprinting to determine the spatial origin of fine sediment in a mountainous river catchment." Earth Surface Processes and Landforms **36**(8): 1072-1089.

Evrard, O., J. Poulenard, J. Némery, S. Ayrault, N. Gratiot, C. Duvert, C. Prat, I. Lefèvre, P. Bonté, M. Esteves (2013). "Tracing sediment sources in a tropical highland catchment of central Mexico by using conventional and alternative fingerprinting methods." Hydrological Processes **27**: 911-922.

Eyrolle, F., S. Charmasson, D. Louvat (2004). "Plutonium isotopes in the lower reaches of the River Rhône over the period 1945–2000: fluxes towards the Mediterranean Sea and sedimentary inventories." Journal of Environmental Radioactivity **74:** 127-138.

Eyrolle, F., D. Louvat, J.-M. Métivier, B. Rolland (2005). "Origins and levels of artificial radionuclides within the Rhône river waters (France) for the last forty years: Towards an evaluation of the radioecological sensitivy of river systems." Radioprotection **40**(4): 435-446.

Eyrolle, F., C. Duffa, C. Antonelli, B. Rolland and F. Leprieur (2006). "Radiological consequences of the extreme flooding on the lower course of the Rhone valley (December 2003, South East France)." Science of the Total Environment **366**(2-3): 427-438.

Eyrolle, F., Claval D., Gontier G. and Antonelli C. (2008). "Radioactivity level in major French rivers: summary of monitoring chronicles acquired over the past thirty years and current status." Journal of Environmental Monitoring **10**: 800-811.

Eyrolle, F., O. Radakovitch, P. Raimbault, S. Charmasson, C. Antonelli, E. Ferrand, D. Aubert, G. Raccasi, S. Jacquet and R. Gurriaran (2012). "Consequences of hydrological events on the delivery of suspended sediment and associated radionuclides from the Rhône River to the Mediterranean Sea." Journal of Soils and Sediments **12**(9): 1479-1495.

Ferrand, E., F. Eyrolle, O. Radakovitch, M. Provansal, S. Dufour, C. Vella, G. Raccasi and R. Gurriaran (2012). "Historical levels of heavy metals and artificial radionuclides reconstructed from overbank sediment records in lower Rhône River (South-East France)." Geochimica et Cosmochimica Acta **82**: 163–182.

Fohrer, N., and L. Chicharo (2011). "Interaction of River Basins and Coastal Waters-An Integrated Ecohydrological View" Reference Module in Earth Systems and Environmental Sciences - Treatise on Estuarine and Coastal Science **10**: 109-150.

Garcia-Orellana, J., J.M. Pates, P. Masqué, J.M. Bruach, J.A. Sanchez-Cabeza, (2009). "Distribution of artificial radionuclides in deep sediments of the Mediterranean Sea." Science of the Total Environment **407**(2):887-898.

Gerbersdorf, S. U., T. Jancke and B. Westrich (2007). "Sediment properties for assessing the erosion risk of contaminated riverine sites. A comprehensive approach to evaluate sediment properties and their covariance patterns over depth in relation to erosion resistance - First investigations in natural sediments at three contaminated reservoirs." Journal of Soils and Sediments **7**(1): 25-35.

Goutelard, F., M. Morello and D. Calmet (1998). "Alpha-spectrometry measurement of Am and Cm at trace levels in environmental samples using extraction chromatography." Journal of Alloys and Compounds **271-273**: 25-30.

Haddadchi, A., D. S. Ryder, O. Evrard, J. Olley (2013). "Sediment fingerprinting in fluvial systems: Review of tracers, sediment sources and mixing models." International Journal of Sediment Research **28**(4): 560-578.

Hodge, V., C. Smith and J. Whiting (1996)."Radiocaesium and Plutonium: Still together in "background" soils." Chemosphere **32**(10): 2067-2075.

Lansard, B., S. Charmasson, C. Gascó, M. P. Antón, C. Grenz and M. Arnaud (2007). "Spatial and temporal variations of plutonium isotopes (^{238}Pu and ^{239,240}Pu) in sediments off the Rhone River mouth (NW Mediterranean)." Science of the Total Environment **376**(1-3): 215-227.

Lau, Y. L. and I. G. Droppo (2000). "Influence of antecedent conditions on critical shear stress of bed sediments." Water Research **34**(2): 663-667.

Le Cloarec, M.-F., P. Bonté, I. Lefèvre, J.-M. Mouchel, and S. Colbert (2007). "Distribution of 7Be, 210Pb and 137Cs in watersheds of different scales in the Seine River basin: Inventories and residence times." Science of the Total Environment **375**: 125-139.

Lee, S.-H., J.J. La Rosa, I. Levy-Palomo, B. Oregioni, M. K. Pham, P. P. Povinec, E. Wyse (2003). "Recent inputs and budgets of ^{90}Sr, ^{137}Cs, $^{239,240}Pu$ and ^{241}Am in the northwest Mediterranean Sea." Deep Sea Research Part II: Topical Studies in Oceanography **50**(17–21): 2817–2834.

Le Roux, G., C. Duffa, F. Vray and P. Renaud (2010). "Deposition of artificial radionuclides from atmospheric Nuclear Weapon Tests estimated by soil inventories in French areas low-impacted by Chernobyl." Journal of Environmental Radioactivity **101**(3): 211-218.

Lefèvre, O., P. Bouisset, P. Germain, E. Barker, G. Kerlau and X. Cagnat (2003). "Self-absorption correction factor applied to ^{129}I measurement by direct gamma-X spectrometry for Fucus serratus samples." Nuclear Instruments and Methods in Physics Research, Section A: Accelerators, Spectrometers, Detectors and Associated Equipment **506**(1-2): 173-185.

Ludwig, W., E. Dumont, M. Meybeck and S. Heussner (2009). "River discharges of water and nutrients to the Mediterranean and Black Sea: Major drivers for ecosystem changes during past and future decades?" Progress in Oceanography **80**(3–4): 199-217.

Masson, O., D. Piga, R. Gurriaran, and D. D'Amico (2010). " Impact of an exceptional Saharan dust outbreak in France: PM10 and artificial radionuclides concentrations in air and in dust deposit." Atmospheric Environment **44**: 2478-2486.

Motha, J.A., P.J. Wallbrink, P.B. Hairsine, R.B. Grayson (2003). "Determining the sources of suspended sediment in a forested catchment in southeastern Australia." Water Resources Research **39**: 1059.

Meybeck, M., H. H. Dürr, S. Roussennac and W. Ludwig (2007). "Regional seas and their interception of riverine fluxes to oceans." Marine Chemistry **106**(1–2): 301-325.

Meybeck, M., L. Laroche, H. H. Dürr and J. P. M. Syvitski (2003). "Global variability of daily total suspended solids and their fluxes in rivers." Global and Planetary Change **39**(1–2): 65-93.

Meybeck, M. and C. Vörösmarty (2005). "Fluvial filtering of land-to-ocean fluxes: from natural Holocene variations to Anthropocene." Comptes Rendus Geoscience **337**(1–2): 107-123.

Miralles, J., O. Radakovitch, J. K. Cochran, A. Véron and P. Masqué (2004). "Multitracer study of anthropogenic contamination records in the Camargue, Southern France." Science of the Total Environment **320**(1): 63-72.

Mitchell, P., J. Sanchez-Cabeza, T. Ryan, A. McGarry, A. Vidal-Quatras (1990). "Preliminary estimates of cumulative caesium and plutonium deposition in the Irish terrestrial environment." Journal of Radioanalytical and nuclear Chemistry **138**(2): 241–256.

Mourier, B., M. Desmet,P.C. Van Metre, B.J. Mahler, Y. Perrodin, G. Roux, J.-P. Bedell, I. Lefèvre, M. Babut (2014). "Historical records, sources, and spatial trends of PCBs along the Rhône River (France)." Science of the Total Environment **476-477**: 568-576.

Navratil, O., O.Evrard, M. Esteves, S. Ayrault, I. Lefèvre, C. Legout, J.-L. Reyss, N. Gratiot, J. Némery, N. Mathys, A. Poirel and P. Bonté (2012). "Core-derived historical records of suspended sediment origin in a mesoscale mountainous catchment: the River Bleone, French Alps." Journal of Soils and Sediments **12**(9): 1463-1478.

Olley, J. M., A. S. Murray, D. H. Mackenzie and K. Edwards (1993). "Identifying sediment sources in a gullied catchment using natural and anthropogenic radioactivity." Water Resources Research **29**(4): 1037-1043.

Ollivier, P., B. Hamelin and O. Radakovitch (2010). "Seasonal variations of physical and chemical erosion: A three-year survey of the Rhone River (France)." Geochimica et Cosmochimica Acta **74**(3): 907-927.

Ollivier, P., O. Radakovitch and B. Hamelin (2011). "Major and trace element partition and fluxes in the Rhône River." Chemical Geology **285**(1-4): 15-31.

Pont, D., J. P. Simonnet and A. V. Walter (2002). "Medium-term changes in suspended sediment delivery to the ocean: Consequences of catchment heterogeneity and river management (Rhône River, France)." Estuarine, Coastal and Shelf Science **54**(1): 1-18.

Radakovitch, O.,V. Roussiez,P. Ollivier,W. Ludwig,C. Grenz andJ.-L. Probst (2008). "Input of particulate heavy metals from rivers and associated sedimentary deposits on the Gulf of Lion continental shelf." Estuarine, Coastal and Shelf Science **77**(2): 285–295.

Raimbault, P. and X. Durrieu de Madron (2003). "Research activities in the Gulf of Lion (NW Mediterranean) within the 1997–2001 PNEC project." Oceanologica Acta **26**(4): 291-298.

Renaud, P., L. Pourcelot, J. M. Métivier and M. Morello (2003). "Mapping of ^{137}Cs deposition over eastern France 16 years after the Chernobyl accident." Science of the Total Environment **309**(1-3): 257-264.

Renaud, P., D. Champion, J. Brenot (2007). "Les retombées radioactives de l'accident de Tchernobyl sur le territoire français : Conséquences environnementales et exposition des personnes." Editions Tec&Doc, Lavoisier, 208 pp.

Rolland, B., 2006. Transfert des radionucléides artificiels par voie fluviale: conséquences sur les stocks sédimentaires rhodaniens et les exports vers la Méditerranée. Ph.D. thesis, University of Paul Cezanne Aix-Marseille, France, 322 pp.

Roussel-Debel, S., P. Renaud and J. M. Métivier (2007). "^{137}Cs in French soils: Deposition patterns and 15-year evolution." Science of the Total Environment **374**(2-3): 388-398.

Sempéré, R., B. Charrière, F. Van Wambeke and G. Cauwet (2000). "Carbon inputs of the Rhône River to the Mediterranean Sea: Biogeochemical implications." Global Biogeochemical Cycles **14**(2): 669-681.

Sicre, M. A., M. B. Fernandes and D. Pont (2008). "Poly-aromatic hydrocarbon (PAH) inputs from the Rhône River to the Mediterranean Sea in relation with the hydrological cycle: Impact of floods." Marine Pollution Bulletin **56**: 1935-1942.

Syvitski, J. P. M. and A. J. Kettner (2007). "On the flux of water and sediment into the Northern Adriatic Sea." Continental Shelf Research**27**(3–4): 296-308.

Syvitski, J. P. M., C. J. Vörösmarty, A. J. Kettner and P. Green (2005). "Impact of Humans on the Flux of Terrestrial Sediment to the Global Coastal Ocean." Science **308**(5720): 376-380.

Thomas, A. J. (1997). "Input of artificial radionuclides to the Gulf of Lions and tracing the Rhone influence in marine surface sediments." Deep-Sea Research Part II: Topical Studies in Oceanography **44**(3-4): 577-595.

Turner, M., M. Rudin, J. Cizdziel and V. Hodge (2003). "Excess plutonium in soil near the Nevada Test Site, USA." Environmental Pollution **125**: 193–203.

Walling, D. E. and A. L. Collins (2008). "The catchment sediment budget as a management tool." Environmental Science & Policy **11**(2): 136-143.
Yeager, K. M. and P. H. Santschi (2003). "Invariance of isotope ratios of lithogenic radionuclides: more evidence for their use as sediment source tracers." Journal of Environmental Radioactivity **69**(3): 159-176.
Zebracki, M., F. Eyrolle-Boyer, A. De Vismes-Ott, C. Antonelli, X. Cagnat and V. Boullier (2013a). "Radionuclide Contents in Suspended Sediments in Relation to Flood Types in the Lower Rhone River." Procedia Earth and Planetary Science **7**: 936-939.
Zebracki, M., F. Eyrolle, X. Cagnat, C. Antonelli, A. De Vismes-Ott and V. Boullier (2013b). "Characterisation of naturally occurring radionuclides in the lower Rhone River (France): Preliminary results from suspended solid monitoring." WIT Transactions on Ecology and the Environment **171**: 235-245.

Figure caption

Figure 1 : Map of the Rhone River catchment. Location of the river monitoring sampling station at Arles and sampling sites of sediment representative of each subcatchment source is indicated. Boundaries of subcatchment areas where the different flood types are generated are also indicated: Oceanic, Cevenol, extensive Mediterranean, and Generalised.

Figure 2 : Boxplot of activities in ^{238}U, ^{232}Th and ^{40}K, in $Bq.kg^{-1}$, in suspended sediment collected in the Lower Rhone River according the four flood types: 1 Oceanic, 2 Cevenol, 3 Extensive Mediterranean, 4 Generalised.

Figure 3 : Boxplot of sediment supply contribution (%) of each sediment source during (a) Oceanic, (b) Cevenol, (c) extensive Mediterranean and (d) generalised floods.

Figure 4 : Suspended sediment load (in 10^6 ton) discharged during floods in the Lower Rhone River between 2001 and 2011 according to the sediment source (a) and the flood type (b).

Figure 5 : Theoretical activity ratio in $^{137}Cs/^{239+240}Pu$ across the Rhone River basin (values decay-corrected to 1/1/2010).

Figure 6 : Plot of $^{239+240}Pu$ vs.^{137}Cs activities, in $Bq.kg^{-1}$ of dry matter, in suspended sediment collected in the Lower Rhone River during floods.

Figure 1

Click here to download Figure: Figure 1 revised.pdf

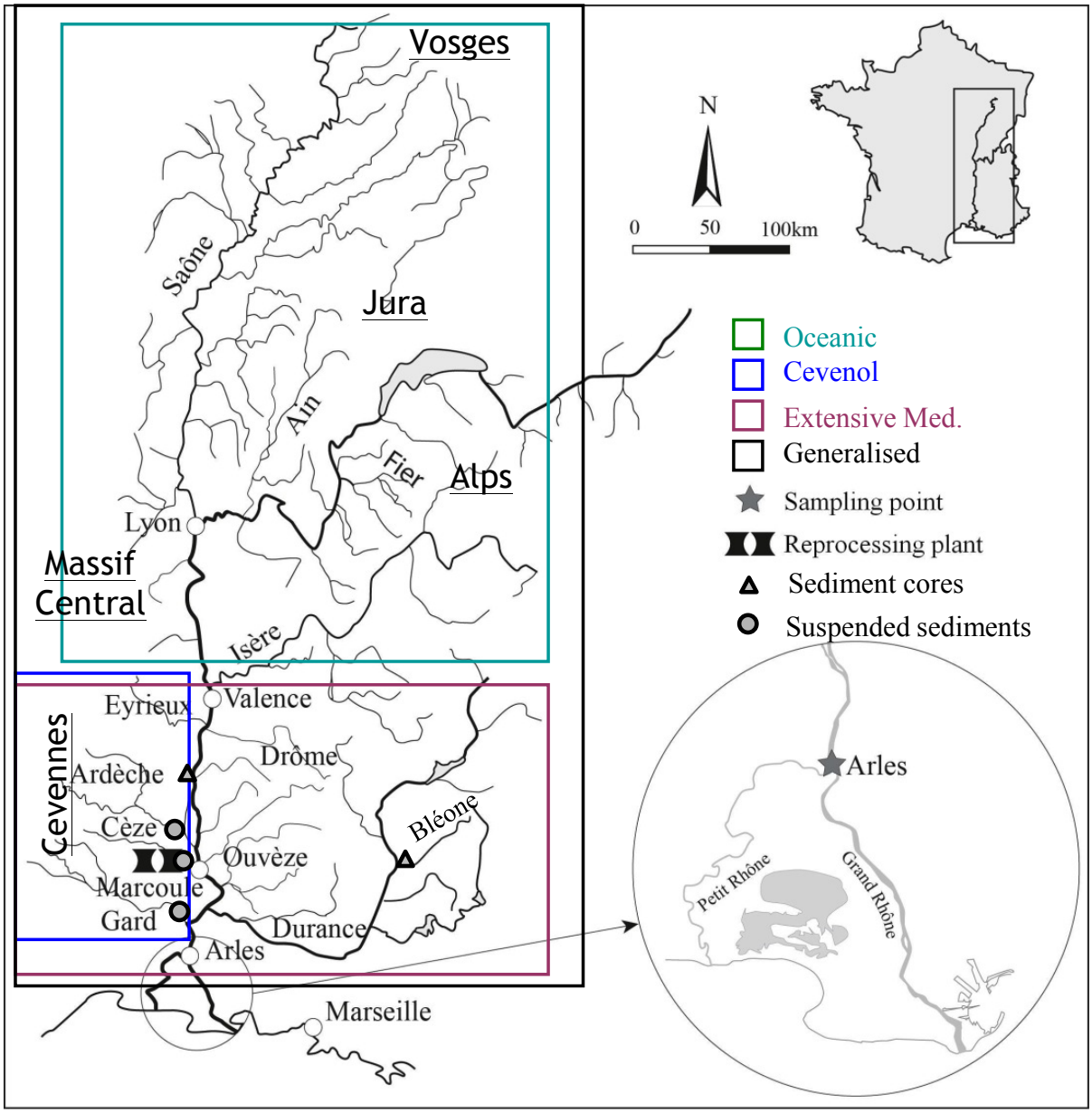

Figure 2

Click here to download Figure: Figure 2 revised.pdf

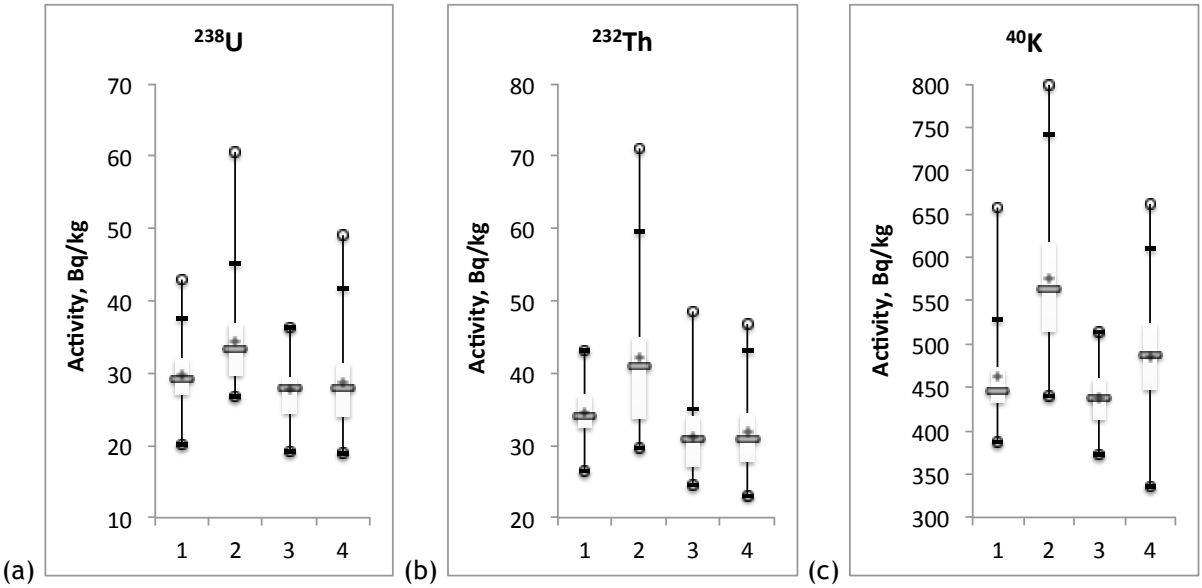

Figure 3

Click here to download Figure: Figure 3 revised.pdf

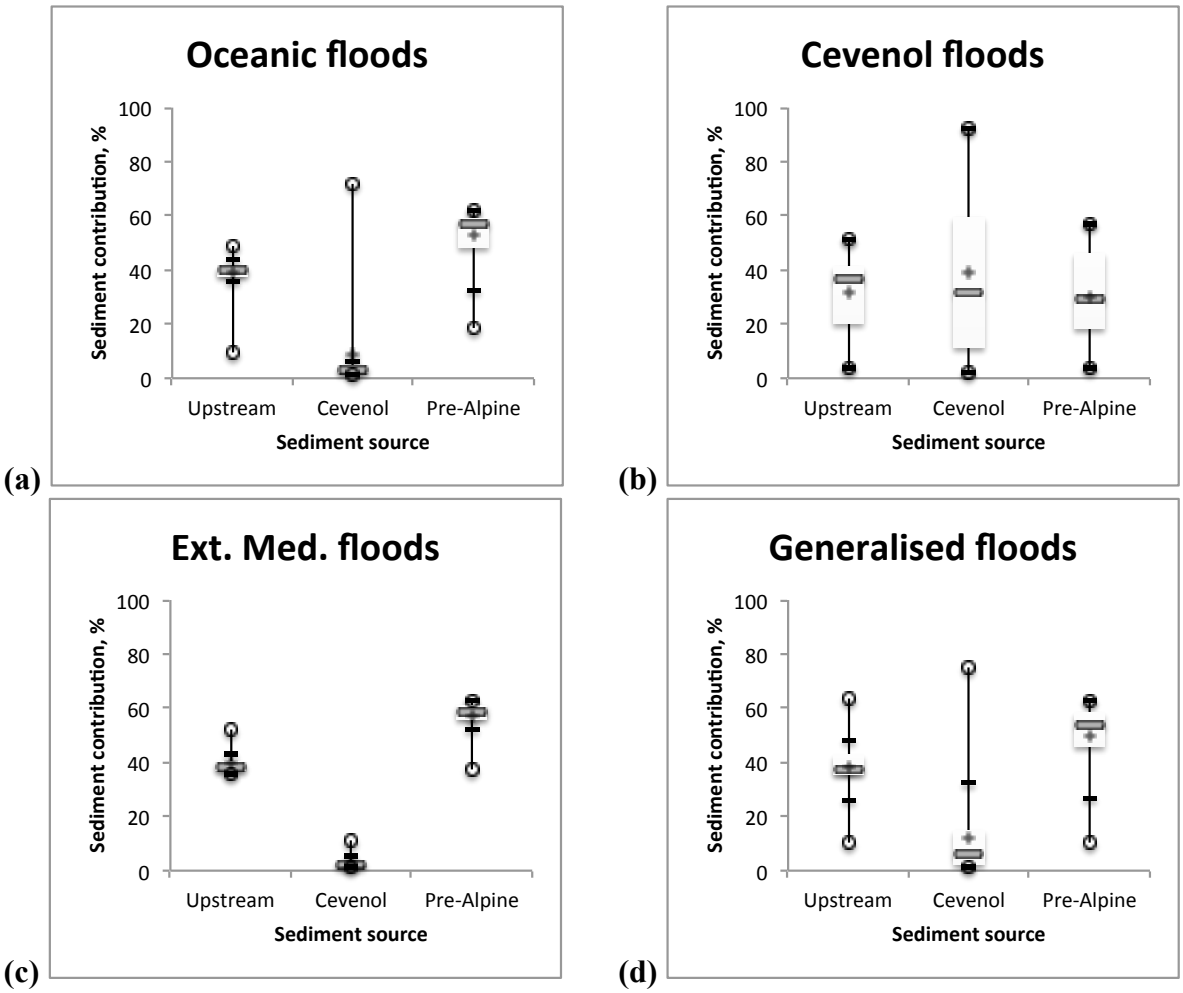

Figure 4

Click here to download Figure: Figure 4 revised.pdf

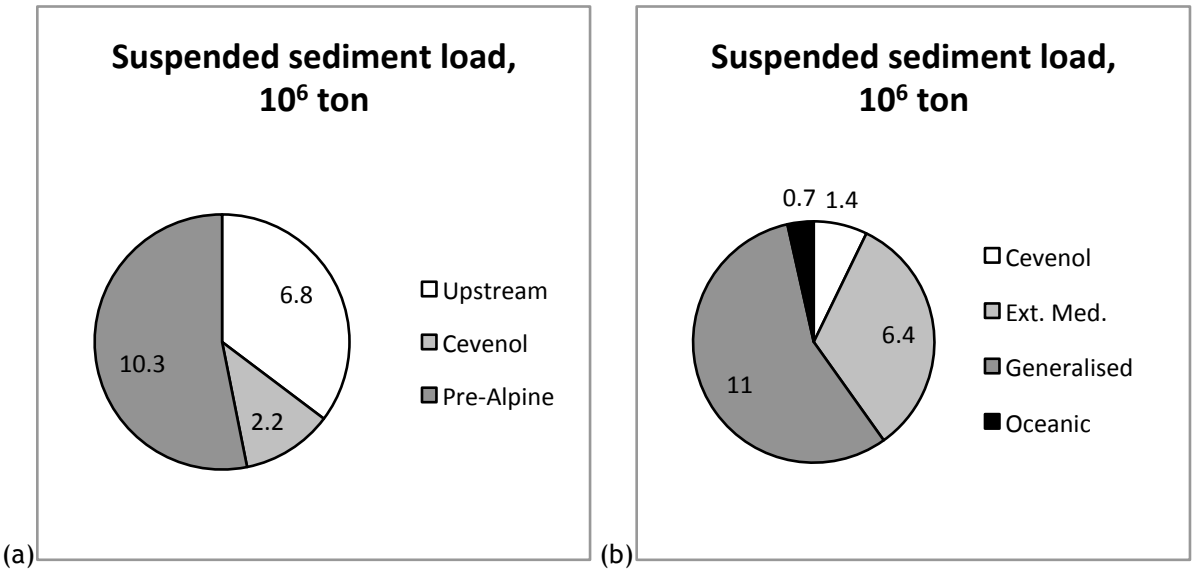

Figure 5

Click here to download Figure: Figure 5 revised.pdf

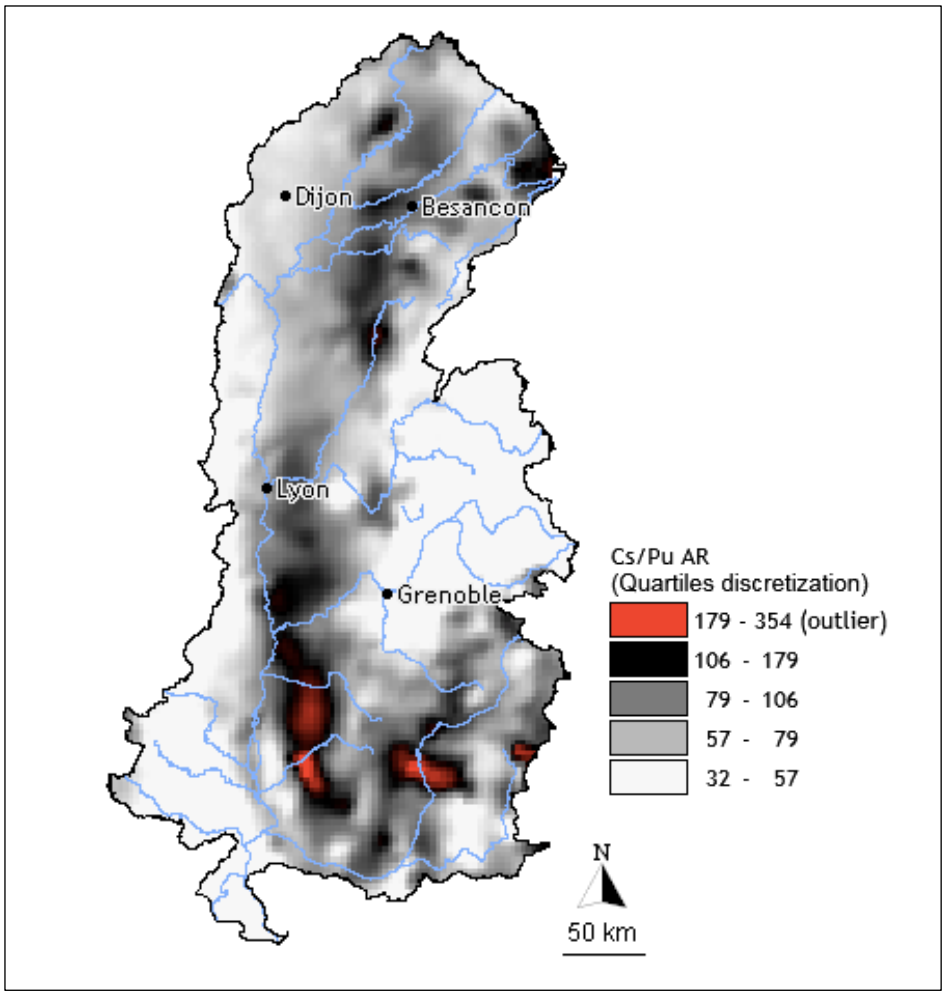

Figure 6

Click here to download Figure: Figure 6.pdf

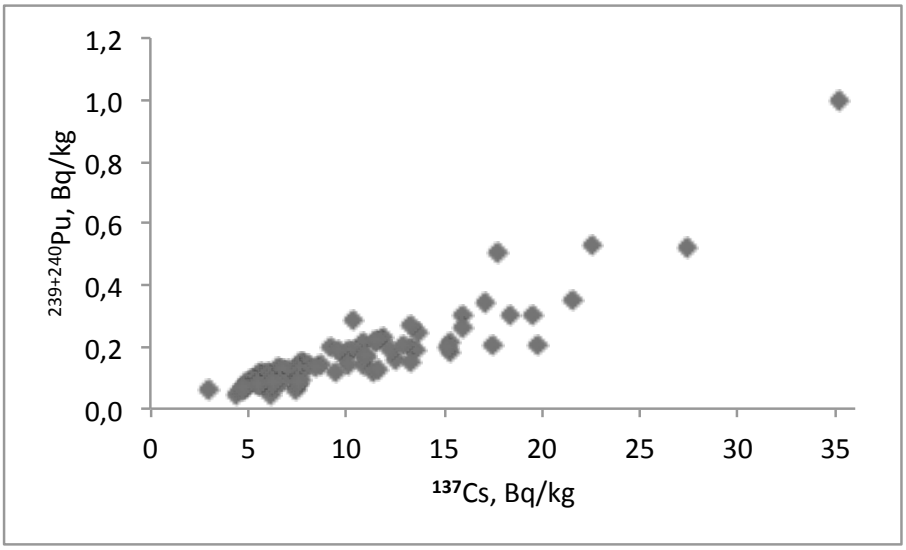

Table caption

Click here to download Table: Table caption revised.pdf

Table 1 : List of investigated flood events, number of collected samples, occurrence of different flood types: Oceanic, Mediterranean, extensive Mediterranean and generalised. The maximum hourly (*daily) water discharge value for each flood event is mentioned between brackets.

Table 2 : Mean radionuclide activities, in $Bq.kg^{-1}$ dry weight, measured in representative sediment source samples collected in each subcatchment.

Table 3 : Activities in ^{238}Pu and $^{239+240}Pu$, $^{238}Pu/^{239+240}Pu$ activity ratio (Pu AR) and Pu isotopes fractions originating from sediment remobilisation downstream of Marcoule, of suspended sediment collected during floods at water discharge exceeding 4,000 $m^3.s^{-1}$ (when direct radioactive releases were forbidden).

Table 4 : Theoretical $^{137}Cs/^{239+240}Pu$ activity ratio in soils of Rhone River subcatchments.

Table 1

Click here to download Table: Table 1 revised.pdf

Flood type	Number of flood events	Number of samples	Flood occurrences (maximum water discharge, in $m^3.s^{-1}$)
Oceanic	11	51	2001: Mar(5828*), Apr(3401*); 2004: Jan(3900); 2005: Apr(3726); 2006: Mar(2978), Apr(3940,3922); 2007: Mar(3452); 2008: Apr(3473), Sep(3134); 2010: Jun(3122); 2012: Jan(3924)
Cevenol	8	50	2002: Sep(9019), 2006: Oct(3225), Nov(4529); 2008: Oct(4178), Nov(5621); 2009: Feb(4046); 2010: May(3540); 2011: Nov(4057)
Extensive Mediterranean	4	25	2003: Dec(9757); 2008: Jan(3318), Apr(3449), Dec(4128)
Generalised	12	89	2000: Nov(3888*); 2002: Nov(9100); 2003: Nov(3577); 2004: Oct(4400); 2006: Dec(3533); 2007: Nov(3302); 2008: May(4310); 2009: Feb(4046), Dec(4401); 2010: Feb(3485), Mar(3670), Dec(3907)
Not defined	2	6	2010: Mar(3012), Sep(2190)

Table 2

Click here to download Table: Table 2 revised.pdf

Sediment source		^{238}U	^{232}Th	^{40}K
Upstream	Number of samples	12	12	12
	Mean activity, $Bq.kg^{-1}$	36	37	512
	sd(1σ)	*6*	*4*	*39*
Pre-Alpine	Number of samples	21	21	21
	Mean activity, $Bq.kg^{-1}$	25	30	486
	sd(1σ)	*4*	*3*	*66*
Cevenol	Number of samples	11	11	11
	Mean activity, $Bq.kg^{-1}$	47	56	674
	sd(1σ)	*12*	*15*	*87*

Table 3

Click here to download Table: Table 3.pdf

Sampling time		Flood type	Discharge $m^3.s^{-1}$	^{238}Pu $Bq.kg^{-1}$ dry	±	$^{239+240}Pu$ $Bq.kg^{-1}$ dry	±	PuAr	±	$^{238}Pu_{Sed}$ %	$^{239+240}Pu_{Sed}$ %
9/10/2002	11:20		7822	0,0138	*0,0020*	0,200	*0,012*	0,069	*0,014*	54	12
9/10/2002	12:25	Cevenol	7189	0,0112	*0,0017*	0,190	*0,011*	0,059	*0,013*	44	9
9/10/2002	13:30		6493	0,0102	*0,0016*	0,168	*0,010*	0,061	*0,013*	46	9
11/19/2002	15:25		7135	0,0305	*0,0132*	0,306	*0,025*	0,099	*0,051*	72	24
11/23/2002	12:15	Generalised	5313	0,0097	*0,0050*	0,208	*0,013*	0,047	*0,027*	26	4
11/26/2002	15:55		9172	0,0339	*0,0087*	0,261	*0,022*	0,130	*0,044*	82	36
12/2/2003	16:40		8060	0,0318	*0,0037*	0,203	*0,011*	0,157	*0,027*	88	46
12/3/2003	11:05	Extensive	10304	0,0488	*0,0056*	0,303	*0,017*	0,161	*0,028*	88	47
12/4/2003	14:00	Mediterranean	9164	0,0216	*0,0029*	0,200	*0,011*	0,108	*0,021*	76	27
12/5/2003	16:25		4220	0,0062	*0,0018*	0,124	*0,009*	0,050	*0,019*	32	5
11/5/2004	13:10	Generalised	4185	0,0450	*0,0060*	0,353	*0,020*	0,127	*0,024*	82	35
5/31/2008	15:00	Generalised	4281	0,0031	*0,0011*	0,081	*0,007*	0,038	*0,016*	5	0,6
5/31/2008	17:00		4264	0,0030	*0,0010*	0,079	*0,006*	0,037	*0,015*	4	0,5
11/2/2008	17:22		4379	0,0099	*0,0021*	0,151	*0,010*	0,066	*0,019*	51	11
11/2/2008	23:09		5373	0,0142	*0,0022*	0,195	*0,011*	0,073	*0,015*	57	14
11/3/2008	06:47		5228	0,0132	*0,0021*	0,176	*0,010*	0,075	*0,016*	59	15
11/3/2008	14:37	Cevenol	4759	0,0093	*0,0017*	0,136	*0,009*	0,068	*0,017*	54	12
11/3/2008	23:55		4604	0,0113	*0,0016*	0,137	*0,008*	0,083	*0,017*	64	18
11/4/2008	07:51		4233	0,0084	*0,0015*	0,124	*0,009*	0,068	*0,017*	54	12
11/4/2008	15:51		4022	0,0055	*0,0012*	0,111	*0,008*	0,049	*0,015*	30	5
2/7/2009	12:37	Generalised	4777	0,0151	*0,0022*	0,134	*0,009*	0,113	*0,023*	77	29
11/5/2011	11:36	Cevenol	4091	0,0216	*0,0021*	0,221	*0,009*	0,097	*0,014*	72	23

Table 4

Click here to download Table: Table 4.pdf

Part of the Rhone basin	Tributary name	Mean	*sd*	Min	Max
Northern	Saone River	88	*27*	39	222
	Isere River	67	*35*	33	201
	Ain River	93	*33*	48	221
	Fier River	44	*6*	36	66
Southern west bank	Aigues River	128	*70*	53	373
	Ouveze River	154	*80*	48	378
	Drome River	136	*52*	59	252
	Durance River	108	*47*	41	358
Southern right bank	Gard River	51	*10*	41	80
	Ceze River	47	*10*	38	99
	Ardeche River	56	*14*	39	118

Supplementary material for on-line publication only

Click here to download Supplementary material for on-line publication only: Supplementary information.pdf